Published in final edited form as:
Cardiovasc Eng Technol. 2011 December 1; 2(4): 276–287. doi:10.1007/s13239-011-0071-5.

Computational Fluid Dynamics and Experimental Characterization of the Pediatric Pump-Lung

Zhongjun J Wu[1], **Barry Gellman**[2], **Tao Zhang**[1], **M Ertan Taskin**[1], **Kurt A. Dasse**[3], and **Bartley P. Griffith**[1]

[1]Artificial Organs Laboratory, Department of Surgery, University of Maryland School of Medicine, Baltimore, MD 21201, USA

[2]Thoratec Corporation, Waltham, MA 02451, USA

[3]Levitronix LLC, Waltham, MA 02451, USA

Abstract

The pediatric pump-lung (PediPL) is a miniaturized integrated pediatric pump-oxygenator specifically designed for cardiac or cardiopulmonary support for patients weighing 5-20 kg to allow mobility and extended use for 30 days. The PediPL incorporates a magnetically levitated impeller with uniquely configured hollow fiber membranes into a single unit capable of performing both pumping and gas exchange. A combined computational and experimental study was conducted to characterize the functional and hemocompatibility performances of this newly developed device. The three-dimensional flow features of the PediPL and its hemolytic characteristics were analyzed using computational fluid dynamics based modeling. The oxygen exchange was modeled based on a convection-diffusion-reaction process. The hollow fiber membranes were modeled as a porous medium which incorporates the flow resistance in the bundle by an added momentum sink term. The pumping function was evaluated for the required range of operating conditions (0.5-2.5 L/min and 1000-3000 rpm). The blood damage potentials were further analyzed in terms of flow and shear stress fields, and the calculations of hemolysis index. In parallel, the hydraulic pump performance, oxygen transfer and hemolysis level were quantified experimentally. Based on the computational and experimental results, the PediPL device is found to be functional to provide necessary oxygen transfer and blood pumping requirements for the pediatric patients. Smooth blood flow characteristics and low blood damage potential were observed in the entire device. The in-vitro tests further confirmed that the PediPL can provide adequate blood pumping and oxygen transfer over the range of intended operating conditions with acceptable hemolytic performance. The rated flow rate for oxygenation is 2.5 L/min. The normalized index of hemolysis is 0.065 g/100L at 1.0 L/min and 3000 rpm.

Keywords

pediatric circulatory support; pediatric cardiopulmonary assist device; pump-oxygenator; computational fluid dynamics; in vitro characterization

Address correspondence and reprint requests to Zhongjun J Wu, PhD, Department of Surgery, University of Maryland School of Medicine, MSTF-436, 10. S. Pine Street, Baltimore, MD 21201, U.S.A., Phone: (410) 706-7715, Fax: (410) 706-7732, zwu@smail.umaryland.edu.

INTRODUCTION

The need for viable mechanical circulatory support devices for young children with advanced heart disease is well established. According to the American Heart Association, about 36,000 babies are born each year with some type of congenital heart defect [1]. As of 2002, the prevalence of congenital heart disease in the United States was estimated to range from 650,000 to 1.3 million. For those pediatric patients who have severe cardiovascular disease and become refractory to conventional therapies, such as medication, aggressive mechanical circulatory intervention may improve the likelihood of survival[2,3]. Historically, extracorporeal membrane oxygenation (ECMO) was the only option for small children experiencing severe heart failure. The survival to discharge for the use of ECMO for cardiac support has remained at 40% to 50% for the past decades and is fraught with complications which increase dramatically with support durations exceeding a few days [4]. Although implantable ventricular assist devices (VADs) have emerged as a safe and effective treatment to improve survival and quality of life for adult patients with heart failure and are routinely used in hospitals for bridge to transplantation, bridge to recovery and cardiogenic shock patients, options remain limited for pediatric patients requiring circulatory support. The Berlin Heart Excor pediatric VAD (Berlin Heart GMBH) device began being employed under emergency use provision in 2002. In the recent US clinical trial of the Berlin Heart Excor device for use in pediatric patients under the US Food and Drug Administration (FDA) Investigational Device Exemption (IDE), the Excor device still has a substantial risk of thrombosis, in particular the 10 cc device intended for children under ~10 kg although the safety and probable benefit have been demonstrated. The MicroMed's DeBakey VAD Child (MicroMed Technology, Inc.) received a Humanitarian Device Exemption approval for use in patients with a BSA (Body Surface Area) > 0.7 m^2, but has encountered severe thrombotic complications.

The lack of chronic pediatric mechanical circulatory support options prompted the National Heart, Lung and Blood Institute (NHLBI) to award contracts to five selected consortiums for the development of novel pediatric circulatory support systems in 2004 [5]. In 2010, the NHLBI awarded four contractors the Pumps for Kids, Infants, and Neonates (PumpKIN) Pre-Clinical Program to bring four promising pediatric circulatory assist devices to human clinical trial. The PediPL device is one of the four PumpKIN devices and was specifically designed for use up to 30 days in patients weighing 5-20 kg. The device is indicated to treat: 1) failure to wean from cardiopulmonary bypass patients who are not sufficiently stable to be moved from the operating room without mechanical circulatory support; 2) children with severe primary respiratory failure or secondary failure associated with cardiac disease, and 3) children with profound cardiogenic shock who require urgent support and may or may not require transition to long-term ventricular assistance.

In the present study, we used a combined computational and experimental approach to characterize the detailed fluid dynamics and functional performance of the PediPL over the intended operating conditions. We also extended our computational fluid dynamics (CFD) based analyses with in-vitro testing to evaluate hemolytic performance of the PediPL. These detailed CFD based analyses and experimental characterization of the functional

performance and **hemocompatibility** provide guidance for the PediPL use and further refinement.

NUMERICAL AND EXPERIMENTAL METHODS

PediPL Design

The PediPL is an extracorporeally placed cardiopulmonary support device and a single-use integrated pump oxygenator. Blood from the failing heart and lungs of a patient is directed to the inlet of the PediPL via an inlet cannula. Blood exits through the outlet port of the PediPL and ultimately return to the patient's circulation through an outlet cannula. The PediPL system is comprised of the single-use PediPL, a motor, a primary drive console, and a set of cannulae (see Figure 1). The PediPL design is based on the previously developed adult size integrated magnetically levitated pump-oxygenator [6,7] and scaled down for the pediatric application. The key required features for the PediPL include the following specifications:

- Durable – The intended duration of use up to 30 days without exchange
- Hemocompatible – Free of thrombus at explant
- Minimal hemolysis – less than 15 mg/dl under normal operation
- Uniform blood flow distribution – minimized areas of stasis
- Competitive hemodynamic capability: 2.5 LPM with 150 mmHg pressure head
- Competitive gas exchange:
    - At least 95% O2 saturation at 2.5 LPM
    - At least 100 ml/min removal of CO2 at 2.5 LPM
    - Small, membrane surface area < 0.3 m^2 and priming volume < 100 ml
- Transportable

Figure 2 shows the flow path of the PediPL on the cross-sectional viewing plane. The pumping function of the PediPL was designed based on the magnetically levitated bearingless impeller/motor technology which was previously implemented in the Levitronix CentriMag® blood pump, a continuous-flow, centrifugal-type rotary blood pump. The magnetic levitation motor and control system used in the PediPL are the same as used for Levitronix CentriMag® blood pump, but the flow path of the PediPL was completely redesigned. The oxygenation component is made of microporous hollow fiber membranes (HFM). To achieve the most effective use of the fiber membranes, maximum gas exchange and elimination of deleterious flow stagnancy, a cylindrical HFM bundle with a patented unique circumferential-radial, uniform outside-in flow path was employed. The dimension of the PediPL is about 116 mm (length) × 97 mm (diameter). The total surface area of the HFM bundle is 0.3 m^2 and the porosity is 0.53, defined as the ratio of the actual volume occupied by the blood to the total volume of the bundle. The priming volume of the device is about 110 ml.

CFD-Based Analysis

The 3D geometry model and computational surface of the PediPL were generated using the 3D computer aided design (CAD) software package (Solidworks, v2006, Solidworks Corporation, Concord, MA, USA). The computational domain encompassed the inlet, outlet, blade-to-blade passages, central opening in the impeller, diffuser channels, manifolds, fiber bundle, and gaps that separate the rotor from the stationary housing wall. The geometry in Parasolid format was imported into a grid-generation software, Gambit v.2.3.16 (Ansys Fluent Inc., Lebanon, NH, USA) where it was preprocessed and meshed into 3D unstructured (UNS) tetrahedral/hybrid elements. Prism layers were implemented on the impeller/rotor surfaces. Controlled mesh was applied in the region between the rotor and stationary housing surfaces, and on the diffuser walls to create a finer mesh structure. The final meshes contained 1.1M nodes and 5.5M computational cells. Finite-volume based CFD solver (Fluent v6.3.26, Ansys Fluent Inc., Lebanon, NH, USA) was utilized to obtain the flow field by solving the governing equations for blood flow within the PediPL. The resolution of the final mesh was determined by running the cases at three different grid resolutions (coarse to fine) to ascertain that the results were grid-independent and converged at a reasonable time.

The rotational motion of the impeller was simulated by the Multiple Reference Frame (MRF) model provided in the Fluent CFD software package. The fiber bundle (blood, fiber walls, and gas phase) was modeled as porous media and the flow behavior through the bundle was approximated by Ergun equation [7]. The permeability and inertial loss coefficient required by the porous media model were treated as isotropic since the porosity or the void ratio of the fiber bundle used in the PediPL device is high (~0.53). The blood oxygenation transport in the hollow fiber membranes was modeled as a convection-diffusion-reaction process. The details of the CFD modeling implementation of the porous media model for simulation of blood flow and oxygen transfer in the fiber bundle can be found in the references [8,9]. The coefficients used in the model for the oxygen transfer simulation were determined experimentally using a mini-oxygenator, which was made of the polymethylpentene microporous hollow fiber membranes (Oxyplus, Membrana, Charlotte, NC, USA) as used in the PediPL. The details of the mini-oxygenator and related oxygen transfer measurements were described previously [9].

Blood was treated as a Newtonian fluid for the CFD simulation. The blood viscosity and density were 0.0035 kg/(m-s) and 1056kg/m^3, respectively. These values were obtained from the measurements of ovine blood with a hematocrit of 35%. Non-slip boundary condition was assumed on the wall. Uniform velocity profile was specified at the inlet of the PediPL, and a pressure-outlet condition was set at the outlet for the flow field simulation. The inlet velocity value was calculated from the corresponding flow rate. The Semi-Implicit Method for Pressure-Linked Equations (SIMPLE) pressure-velocity coupling algorithm was utilized with the pressure staggering option (PRESTO) on the pressure. Second order upwind scheme was selected for the solutions of momentum, turbulence, and scalar transport equations. Steady laminar flow was assumed for low flow rates (0.5 to 1.5 LPM) while the SST k-w turbulence model was utilized for high flow rates (2.0 to 2.5 LPM). The Reynolds number, calculated based on the inlet diameter and velocity, was used to

determine the Laminar or Turbulent assumption. The flow was considered as Laminar for the flow rates with Reynolds number of 1000 and below, whereas turbulence model applied to the higher flow conditions. The similar criterion was used for CFD modeling of blood pumps in the literature, as previously summarized [10]. The SST k-w turbulence model requires fine near-wall mesh structure, and this was established with narrow prism layers attached to the walls of the PediPL model. This provided a mean value of 2.5 for the dimensionless distance parameter, y+ which ensured the required near-wall resolution within the viscous sublayer.

The hemolytic blood damage potential was calculated by Eulerian approach, in which the hemolysis index was predicted by solving a scalar transport equation [11]. The scalar quantity and the source term were derived from the power-law equation to determine flow induced hemolysis from shear stress level and exposure time. The coefficients for the power law equation were obtained by fitting the above power law equation to experimentally measured hemolysis data with bovine blood [12], which was used for the in-vitro experimental characterization of the PediPL device.

The hemolysis index and oxygen transfer models were programmed in user-defined subroutines (UDF) and user-defined scalars (UDS) and then compiled into the Fluent CFD solver. The oxygen transfer model was coupled with continuity and momentum equations in the Fluent CFD solver to solve the velocity and pressure fields, gas transfer, oxygen partial pressure, and oxygen saturation. The hemolysis model was solved as a post-processing procedure after the flow field solution was obtained. The computations were carried out on a PC workstation with two Intel Xeon quad-core 2.66GHz CPUs and 16.0 GB RAM with the Windows XP 64 bit operating system.

In-Vitro Evaluation: Hydrodynamics, Oxygen Transfer and Hemolysis

The hydrodynamic performance of the PediPL was evaluated in a circulatory loop using ovine blood. The flow loop was comprised of a PediPL device, blood reservoir, and the resistor. Fresh ovine blood with 35% hematocrit at 37°C was used as the working fluid. Pressures at the inlet and outlet of the PediPL were measured at different flow rates (0 to 2.5 L/min) at five rotating speeds (1000, 1500, 2000, 2500 and 3000 rpm) using a calibrated piezoelectric pressure transducer (Model 1502B01EZ5V20GPSI, PCB Piezotronics, Inc., Depew, NY, USA). For each speed setting, the flow rate was adjusted by changing the afterload resistance of the flow loop using a C-clamp and measured with a calibrated ultrasonic flow meter (TS410, Transonic Systems, Inc., Ithaca, NY, U.S.A.) with a H9XL tubing probe. The difference between them was calculated to represent the device generated pressure head.

The oxygen transfer performance of the PediPL was tested in an experimental blood flow circuit according to the protocol for evaluating cardiovascular implants and artificial organs-blood gas exchangers (oxygenators) specified in ISO standard 7199 [13]. Fresh ovine blood with 35% hematocrit was used. Temperature was maintained at 37°C and data were collected at the flow rates from 0.5 to 3.0 L/min at a rotating speed of 3000 rpm. The experiments were performed under an oxygen gas flow to blood flow ratio at 1:1. Pure oxygen was used as the sweep gas and the O2 saturation at the inlet of the PediPL was set

around 64%. The circulating blood was first pre-conditioned in the circulating loop to the normal venous blood condition as specified in the ISO standard. Then the oxygen transfer test was initiated by switching the circulatory flow loop into a single-pass flow loop and changing the returning blood from the PediPL to a separate reservoir. Blood samples were collected at the inlet and outlet of the PediPL device and analyzed with a blood gas analyzer (Stat Profile Phox Plus L, Nova Biomedical, Waltham, MA, U.S.A.). The oxygen transfer rate was calculated based on the measured O2 partial pressure and O2 saturation of the blood samples at the inlet and outlet using the standard method [6].

The level of device-induced hemolysis by the PediPL was tested in an in-vitro circulatory flow loop using ovine blood. The in-vitro test was conducted under two operating conditions (1.0 L/min at 3000 rpm and 2.5 L/min at 3200 rpm) according to the recommended practice for assessment of hemolysis for continuous flow blood pumps specified by the American Society of Testing and Materials (ASTM F1841-97) [14]. Fresh ovine blood (hematocrit: 30%) at 37 °C was circulated for 3 hours. Blood samples were collected every 30 minutes for the measurement of plasma free hemoglobin (PFH). Details of blood collection and preparation, measurement of PFH, and experimental procedures have been described previously [12].

RESULTS

Computational results of the pumping function, gas transfer, and **hemompatibility** of the PediPL, obtained using the flow simulation methods described, are presented in the following sections in conjunction with the experimental performance evaluations.

Hydrodynamic Pumping Performance of the PediPL

The hydrodynamic pumping function of the PediPL is presented in Figure 3. The pumping function is expressed as the pump-generated pressure head (difference between the pressures at outlet and inlet) versus flow curves (H-Q curves) at a specific rotational speed. The CFD simulations were performed at three rotational speeds (flow rate: 0.5 ~ 2.0 L/min). The experimental measurements were conducted at five rotational speeds (flow rates: 0.5 ~ 3.0 L/min). A continuous decrease in the pressure head with increasing flow rate at a specified rotating speed was observed. The computationally predicted pressure heads at these operating conditions were found in good agreement with the experimentally measured data. The average difference between the numerical and experimental results of the pressure head is 7.2 ± 4.0 mmHg. Based on the pediatric blood pressure data from the NIH clinical center, the body weight data of the pediatric population from the US the Centers for Disease Control and Prevention, and the published relationship between the body mass and cardiac output in children [15], an expected pressure versus flow curve for pediatric circulatory support was also plotted in Figure 3 (shaded box curve). In this curve, we also considered the pressure losses in the inflow cannula (14 Fr. to 20 Fr.), the outflow cannula (12 Fr. to 16 Fr.) and connection tubing. We have designed the PediPL to perform optimally at an average pressure differential of 110 mmHg over the target ranges of flow (500 cc-2500cc/min) for 3.0-25kg children. Both experimental and numerical results have shown that the hydrodynamic performance of the PediPL meets the requirements and the PediPL can

provide adequate blood flow over a range of physiological conditions for pediatric patients by adjusting the operating speed.

Pressure and Flow Patterns

Figure 4 shows the pressure distributions on the central cut plane through the inlet/outlet (a), and at the surfaces of impeller-diffuser (b) at a flow rate of 1 L/min and an impeller rotating speed of 3000 rpm (Q=1 L/min, ω=3000 rpm). As expected, flow enters the inlet with lower pressure **(set as 0 mmHg at the inlet)** as shown in Fig. 4a, the static pressure is gradually increased (Fig. 4b) with the imparted momentum from the rotating impeller. The pressure head is generated by the impeller blades, and the dynamic pressure is converted to static pressure at the blade tips and diffuser fins (Fig. 4b). The pressure decreases from the outer surface to the inner surface of the fiber bundle by 2-4 mmHg as the blood passes through the fiber bundle. The blood exits at the outlet connector of the device through the annular gap between the inner and the outer surfaces of the pump inlet guide without losing significant amount of the generated pressure (< 10 mmHg). This further shows the hydrodynamic efficiency of the current configuration. **The pressure head at the outlet is 175 mmHg.**

Figure 5 shows the sectional view of the velocity field on the central cut plane of the PediPL and near wall velocity vectors on the impeller wall at Q=1 L/min, ω=3000 rpm. Flow enters the pump chamber from the inlet and diverts 90 degree into the impeller blade passages due to the centrifugal forces. Afterwards, flow is guided out by the diffuser fins into the space between the housing wall and the outer surface of the fiber bundle. The velocity fields show that the blood flows through the fiber bundle radially and rather uniformly across the fiber bed from top to bottom. The near wall velocity vectors on the impeller/rotor of the PediPL shows that well distributed vectors exist on the impeller blades as well as good surface washing on the rotor surface.

The velocity field at the middle-blade cut through the impeller blades/diffuser fins is shown in Figure 6 for the same operating condition (Q=1 L/min, ω=3000 rpm). In Figure 6, the velocity vectors are plotted with color mapped magnitude and fixed length arrows. Well streamlined flow features inside the impeller passages and at the interface between impeller and diffuser can be noticed. On the enlarged view of an arbitrary section (Figure 6(b)), there are some disturbances at the diffuser passages. However, well guided flow distribution is seen, indicating a very compatible diffuser structure with the impeller blade structure. Figure 6 also shows no localized small vortexes or flow disturbances at the impeller eye (center opening portion of the impeller), indicating a good guided and aligned flow from the inlet to the central impeller opening.

The flow patterns at other operating conditions are similar to those at 1.0 L/min and 3000 rpm. The velocity magnitude varied in the inlet, impeller region and fiber bundle with the impeller rotational speed and flow rate. At the same rotational speed, major difference in the flow patterns between different flow rates was noticed at the sections between the blade tip and diffuser leading edge. At 0.5 L/min and 3000 rpm, there was flow separation at the trailing edge of the suction of the diffuser fins. At 2.5 L/min and 3000 rpm, small recirculation areas was observed at the suction side of the leading edge of the diffuser fins.

Oxygen Transfer Performance

The simulated oxygen saturation (SO_2) distribution of ovine blood in the PediPL is presented in Figure 7 (a) along with the in-vitro measured inlet and outlet values at a blood flow of 1 L/min at a rotational speed of 3000 rpm. Pure oxygen was assumed in the lumen of the hollow fibers. The experiments were performed under an oxygen gas flow to blood flow ratio of 1:1. As can be seen, the blood enters the device with uniform low oxygen saturation level, and moves towards the outer surface of the HFM bundle without any change in the oxygen saturation level. When blood passes through the fiber bundle, it becomes gradually oxygenated. As the blood penetrates radially deep into the fiber bundle, the blood oxygen saturation increases, and the blood is almost fully saturated at the outlet (>98%). The measured oxygen saturation at the outlet was well comparable to the predicted value under the same inlet conditions. The oxygen saturation across the fiber bundle is uniformly distributed from the bottom to top of the HFM bundle. The predicted oxygen transfer rates with in-vitro experimentally measured data at different flow rates are shown in Figure 7 (b). The oxygen transfer rate increases with the increase in flow rate. Additionally, computationally predicted oxygen transfer performance was in excellent agreement with the in-vitro experimentally measured data. The required oxygen transfer versus body weight for children is also shown in Figure 7 (b). Table 1 lists the rated flow and membrane surface area of the PediPL and other pediatric oxygenators currently on market.

Hemolytic Performance

The shear stress distribution at the central cut plane is presented in Figure 8 (a). The distribution of different shear stress levels is shown in a histogram plot in **Figure 8 (b)** regarding each computational cell volume. The shear stresses in the majority of the flow domain do not exceed the shear stress threshold level (~100 Pa, [16]) at a flow rate of 1 L/min at an impeller rotating speed of 3000 rpm. The higher shear stresses are only seen in the region close to the impeller blades and diffuser fins, and for the rest of the domain the shear stresses are very low. Furthermore, the contribution of the high shear stress field to the overall device volume is very insignificant (Fig. 8(b) and (c)). Close examination indicates that most of the flow domain will locate in lower shear stress regions, and unlikely to cause excessive flow-induced blood damage.

The hemolysis index (HI) distributions through the central planar cut view and on the impeller/rotor surface of the PediPL at a flow rate of 1 L/min at a rotational speed of 3000 rpm is presented in Figure 9. It can be seen that blood enters the device without any hemolysis, and exits with a certain degree of increase. The highest hemolysis is observed at the bottom of the device around the rotor. To couple the hemolysis observations to the flow field, the vector fields colored by the HI values are presented in Figure 9 (c) on the central cut plane. In the figure white guidance arrows are drawn to emphasize the significant flow features. The relatively higher HI region through the second half of the inlet tube is created by the reversed flow field observed on that region. The highest HI region was noticed around the rotor section. Although it was noticed that there was a slightly increase in HI, the value was insignificant. The computationally predicted HI values are 0.0080% and 0.0029%, respectively, for the flow rates at 1.0 LPM and 2.5 LPM at the rotational speed of 3000 rpm.

Accordingly, we performed in-vitro hemolysis tests in the circulatory flow loop. About 1.3 liters of fresh ovine blood with the hematocrit of 30% was circulating in the flow loop for 3 hours for the blood flow rates of 1.0 and 2.5 L/min, respectively. Blood samples were drawn from the flow loop every 30 minutes and the plasma free hemoglobin (PFH) value is measured for each sample. Then the normalized index of hemolysis (NIH) was calculated based on the multiple measurements. Averaged In-vitro measured NIH was ~ 0.065 for Q =1 L/min at ω = 3000 rpm and 0.04 for Q =2.5 L/min at ω = 3200 rpm. The experimental NIH value demonstrated that the PediPL has excellent hemolytic performance under the targeted physiological operating condition (1 to 2.5 L/min against 150 mmHg pressure head). These values are comparable to the typical NIH values for circulatory assist devices tested in our laboratory. Table 2 lists the hemolysis data of the PediPL with other circulatory assist devices and integrated pump-oxygenators currently on market or under development.

DISCUSSION

Design and development of the pediatric pump-lung (PediPL) is the same as those for any other blood contacting devices. It always starts with a concept with that the intended functionality is realized for the specified use of a device. Computational modeling has been used for decades in engineering for analyzing or predicting performance and function of aircrafts and hydrodynamic machinery in the design and development process. The application of CFD to blood contacting devices is relatively new, but has enormous potential in optimizing the functional characteristics and hemocompatibility of these devices. With the detailed 3D flow information, regions of high shear stress, recirculation and stagnant flow can be identified. These flow features can be used semi-quantitatively to illustrate relationships between fluid dynamics and clinical complications and have provided certain degree of guidance for improvement and safe operation of these devices. Almost all recently developed rotary-pump-based ventricular assist devices (VADs) have undergone CFD analysis. Additionally, some older VAD designs are being re-evaluated using CFD. These previous works have demonstrated the potentials and benefits of computational modeling as an emerging and promising tool for modeling and analysis of blood flow in blood pumps, heart valves, oxygenators and cardiovascular system.

In the present study, the PediPL was designed based on the previously developed adult size maglev pump-oxygenator [6]. The impeller and magnetically levitated motor technology were directly adapted from the previously developed CentriMag (R) blood pump. However, the PediPL is no longer a simple centrifugal blood pump. It has a uniquely configured flow path required to achieve the most effective use of the fiber membranes, maximum gas exchange and elimination of deleterious flow stagnancy. A cylindrically HFM bundle with the circumferential-radial uniform outside-in flow path is employed. Thus the blood flow exiting from the pump chambers is distributed 360 degree around and enter into the hollow fiber membranes. To avoid the expense of repeated construction of prototypes and in vitro experimentation, we first utilized CFD-based design and analysis approach to characterize the functional performance (blood pumping and gas transfer) and blood damage potential (flow patterns, shear stress distribution and hemolysis index). The PedPL was evaluated virtually from the geometrical construction to prediction of functional performance to

evaluation of hemocompatibility before the physical prototype was fabricated and tested in-vitro.

Both the CFD and in-vitro results have demonstrated that the PediPL met the special requirements for pediatric circulatory/cardiopulmonary support. These data clearly show that the PediPL not only functions as a blood pump, but also serves as a gas transfer device. The PediPL was able to pump blood at a flow rate of 3 liter/min against a 140 mmHg pressure head at the rotational speed of 3000 rpm and to deliver about 150 ml O_2/min (normalized: ~500 ml/min/m^2). The normalized oxygen transfer rate has already outperformed all commercially available blood oxygenators on per unit fiber surface basis (see Table 1). For circulatory support, a 5 kg or 20 kg child will require a basal flow of 750 ml/min (150 ml/min/kg) or 2,500 ml/min (125 ml/min/kg). For cardiopulmonary support, the oxygen transfer requirement will be 31 ml O_2 for a 5 kg child, assuming a body surface area (BSA) of 0.25 m^2 (@125 kg/m^2,) and 88 ml O_2 for a 25 kg child (BSA: 0.68 m^2). Thus the functional performance of the PediPL meets the circulatory or cardiopulmonary support requirements for use in pediatric patients weighing 5 kg to 25 kg.

In addition to the functional performance, i.e., blood pumping and oxygen transfer, the hemolytic performance of the PediPL was also characterized. The blood damage potential was assessed by analyzing the flow derived shear stress field and flow-induced hemolysis. The localized hotspots of higher shear stresses were found on the impeller tips and the gap between the rotor and housing wall. However, the stress histogram indicated that only a very small portion of the flow domain experienced higher shear stresses under the intended operating conditions (0.5 to 2.5 LPM against 100 mmHg head). To further evaluate the hemolytic performance of the PediPL, in-vitro hemolysis testing was carried out at two operating conditions (1.0 LPM at 3000 rpm, and 2.5 LPM at 3200 rpm). The NIH values for the PediPL seemed to be a bit high. This may be because we used ovine blood for the experiment. From our own data and published data by others, the ovine red blood cells are more fragile and susceptible to damage compared to bovine blood which are often used in the hemolysis testing [22]. We have used both ovine and bovine blood to test the Levitronix CentriMag $^{(R)}$ blood pump. The NIH value produced by the CentriMag $^{(R)}$ blood pump was 0.0029 g/100L for bovine blood while it was 0.036 g/100L for the same operating condition (see table 2). Thus the NIH values induced by the PediPL are acceptable and comparable to the NIH values induced by the adult size pump-oxygenator [6], the CentriMag$^{(R)}$ blood pump and other blood pumps (see Table 2). When comparing the HI values obtained from the computational simulation to the experimental results, the computational prediction was slightly over-estimated (0.0080% vs.0.0030% for 1.0 LPM at 3000 rpm). It is suggested that the further development of a hemolysis model is needed.

In addition to oxygenators and blood pumps, efforts are also devoted to development of integrated pump-oxygenators for circulatory or cardiopulmonary support. The approaches include mating a blood pump serially to an oxygenator, placing a rotating impeller within a fiber bundle and rotating a fiber bundle itself. The demised CardioVention CORx system was a miniaturized cardiopulmonary bypass system in which a centrifugal pump was placed underneath the fiber bundle and the outlet of the pump was directly fused to the housing of the fiber bundle. The CORx system was used briefly for adult cardiopulmonary bypass

during cardiac surgical procedures, but not available now. The membrane surface area of the CORx is 1.2 m^2 and the rated flow is and 6.0 L/min. The CORx system is capable of pumping blood against 230 mmHg pressure head. A highly integrated extracorporeal membrane oxygenator (HEXMO) is being developed at the RWTH Aachen University [23]. Two prototypes of the HEXMO have been fabricated and tested. One prototype with a membrane surface area of 0.9 m^2 was tested in pigs. The prototype device was operated to generate a flow of 1.5 to 1.6 L/min. It is interesting to note that the device did not fully saturate the entering venous blood and returned the blood with 90 to 92 % oxygen saturation. The other prototype device of the HEXMO with a membrane surface area of 0.36 m^2 was tested in vitro and in rabbits [24]. The maximum achievable blood flow rate is 700 ml/min and the oxygen transfer rate is about 48 ml/min. Although the hemolysis test was carried out, only the increase of plasma free hemoglobin with time was reported. The NIH value was not calculated. The pediatric cardiopulmonary assist system (pCAS) from Ension is another integrated pediatric pump-oxygenator under development. Blood flow rates of up to 1.2 L/min and oxygenation saturation levels of 100% were achieved with the use of 10 Fr. venous and 8 Fr. arterial cannulae in piglets [25]. However, technical details and performance data of pCAS have not been published. In parallel with these efforts, we have previously developed an adult bed-side pump-oxygenator with a magnetically suspended impeller and a unique flow path [6]. Compared to those devices under the development, we used only a membrane surface area of 1.0 m^2 to achieve fully basal adult respiratory or cardiopulmonary support. Based on the unique circumferential-radial, uniform outside-in flow path and the similar magnetically bearingless motor technology, the PediPL was developed with a membrane surface area of 0.3 m^2. We are able to achieve a rated flow of 2.5 L/min with a prime volume of 110 ml for the PediPL. The hemolytic performance of the PediPL is comparable to that of clinically used circulatory assist devices.

CONCLUSION

We have designed a pediatric pump-lung device for circulatory or cardiopulmonary support for young patients weighing 5 to 25 kg. The functional performance and **hemocompatibility** were characterized using a combined computational and experimental approach. The data indicate that the PediPL is capable of providing necessary oxygen transfer and blood pumping requirements for pediatric patients. Smooth blood flow characteristics and low blood damage potential were observed in the entire device. The in-vitro tests further supported that the PediPL can provide adequate blood pumping and oxygen transfer over the range of intended operating conditions with acceptable hemolytic performance.

Acknowledgments

This study was supported in part by the National Institutes of Health (Contract Number: HHSN268201000014C and Grant Numbers: R42HL084807, R01HL082631, R01 HL 088100).

REFERENCES

1. American Heart Association. Congenital Cardiovascular Defects – Statistics. 2009.

2. Duncan BW, Bohn DJ, Atz AM, French JW, Laussen PC, Wessel DL. Mechanical circulatory support for the treatment of children with acute fulminant myocarditis. J Thorac Cardiovasc Surg. 2001; 122:440–448. [PubMed: 11547292]
3. Bartlett RH. Extracorporeal Life Support: History and New Directions. Seminars in Perinatology. 2005; 29:2–7. [PubMed: 15921146]
4. Haines NM, Rycus PT, Zwischenberger JB, Bartlett RH, Undar A. Extracorporeal Life Support Registry Report 2008: Neonatal and Pediatric Cardiac Cases. ASAIO J. 2009; 55:111–116. [PubMed: 19092657]
5. Baldwin JT, Borovetz HS, Duncan BW, Gartner MJ, Jarvik RK, Weiss WJ, Hoke TR. The National Heart, Lung, and Blood Institute Pediatric Circulatory Support Program. Circulation. 2006; 113:147–55. [PubMed: 16391168]
6. Zhang T, Cheng G, Koert A, Zhang J, Gellman B, Yankey GK, et al. Functional and biocompatibility performances of an integrated Maglev pump-oxygenator. Artif Organs. 2009; 33:36–45. [PubMed: 19178439]
7. Ergun S. Fluid flow through packed columns. Chemical Engineering Progress. 1952; 48:89–94.
8. Zhang J, Taskin ME, Koert A, Zhang T, Gellman B, Dasse KA, et al. Computational design and in vitro characterization of an integrated maglev pump-oxygenator. Artif Organs. 2009; 33:805–17. [PubMed: 19681842]
9. Zhang J, Nolan TDC, Zhang T, Griffith BP, WU ZJ. Characterization of membrane blood oxygenation devices using computational fluid dynamics. Journal of Membrane Science. 2007; 288:268–279.
10. Fraser KH, Taskin ME, Griffith BP, Wu ZJ. The Use of Computational Fluid Dynamics in the Development of Ventricular Assist Devices. Med Eng Phys. 2011; 33:263–80. [PubMed: 21075669]
11. Taskin ME, Zhang T, Gellman B, Fleischli A, Dasse KA, Griffith BP, et al. Computational Characterization of Flow and Hemolytic Performance of the UltraMag (™) Blood Pump for Circulatory Support. Artificial Organs, 2010. Dec; 2010 34(12):1099–113.
12. Zhang T, Taskin ME, Fang HB, Pampori A, Jarvik R, Griffith BP, et al. Study of Flow-induced Hemolysis using Novel Couette-Type Blood-Shearing Devices. Artif Organs. Aug 2.2011 doi: 10.1111/j.1525-1594.2011.01243.x. [Epub ahead of print] PMID: 21810113.
13. International Organization for Standardization. ISO 7199: Cardiovascular implants and artificial organs-blood gas exchangers (oxygenators). 1st edition. 1996.
14. American Society for Testing and Materials. 2004. ASTM F1841-97: Standard Practice for Assessment of Hemolysis in Continuous Flow Blood Pumps.
15. de Simone G, Devereux RB, Daniels SR, Mureddu G, Roman MJ, Kimball TR, et al. Stroke Volume and Cardiac Output in Normotensive Children and Adults: Assessment of Relations With Body Size and Impact of Overweight. Circulation. 1997; 95:1837–1843. [PubMed: 9107171]
16. Blackshear, PL. Mechanical hemolysis in flowing blood, in Biomechanics: Its Foundation and Objectives. In: Fung, YC., editor. Prentice-Hall; Englewood Cliffs, NJ: 1972. p. 501-528.
17. Zhang J, Gellman B, Koert A, Dasse KA, Gilbert RJ, Griffith BP, et al. Computational and experimental evaluation of the fluid dynamics and hemocompatibility of the CentriMag blood pump. Artif Organs. 2006; 30:168–77. [PubMed: 16480391]
18. James NL, Wilkinson CM, Lingard NL, Van der Meer AL, Woodard JC. Evaluation of hemolysis in the ventrassist implantable rotary blood pump. Artif Organs. 2003; 27:108–13. [PubMed: 12534722]
19. Svitek RG, Smith DE, Magovern JA. In vitro evaluation of the TandemHeart pediatric centrifugal pump. ASAIO J. 2007; 53:747–53. [PubMed: 18043160]
20. Kawahito S, Maeda T, Motomura T, Ishitoya H, Takano T, Nonaka K, et al. Hemolytic characteristics of oxygenators during clinical extracorporeal membrane oxygenation. ASAIO J. 2002; 48:636–9. [PubMed: 12455774]
21. Svitek RG, Frankowski BJ, Federspiel WJ. Evaluation of a pumping assist lung that uses a rotating fiber bundle. ASAIO J. 2005; 51:773–780. 2005. [PubMed: 16340367]

22. Jikuya T, Tsutsui T, Shigeta O, Sankai Y, Mitsui T. Species differences in erythrocyte mechanical fragility: comparison of human, bovine, and ovine cells. ASAIO J. 1998; 44:M452–5. [PubMed: 9804471]

23. Kopp R, Bensberg R, Arens J, Steinseifer U, Schmitz-Rode T, Rossaint R, et al. A miniaturized extracorporeal membrane oxygenator with integrated rotary blood pump: preclinical in vivo testing. ASAIO J. 2011; 57:158–63. [PubMed: 21317635]

24. Arens J, Schnoering H, Pfennig M, Mager I, Vázquez-Jiménez JF, Schmitz-Rode T, et al. The Aachen MiniHLM--a miniaturized heart-lung machine for neonates with an integrated rotary blood pump. Artif Organs. 2010; 34:707–13. [PubMed: 20883389]

25. Baldwin JT, Borovetz HS, Duncan BW, Gartner MJ, Jarvik RK, Weiss WJ. The national heart, lung, and blood institute pediatric circulatory support program: a summary of the 5-year experience. Circulation. 2011; 123:1233–40. [PubMed: 21422399]

(a) (b)

Figure 1.
The PediPL device. (a) Photograph of fully assembled device with cannulae; (b) Control console.

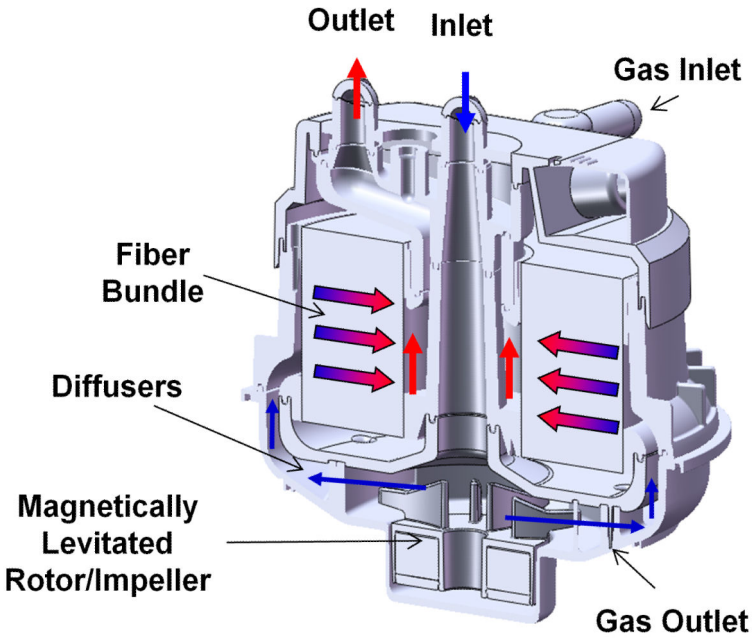

Figure 2.
Cross sectional diagram depicting the relationship of the pump and oxygenator components and flow path.

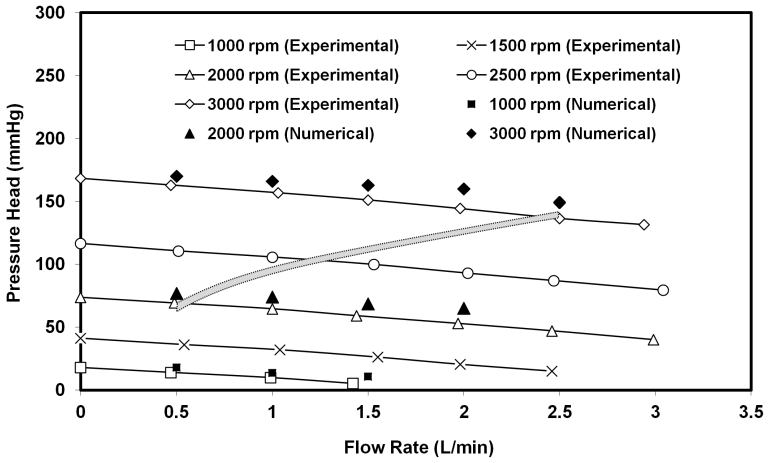

Figure 3.

H-Q curves for the PediPL. Both experimental and numerical data are plotted together. Shaded area suggests targeted operating range expected for young patients.

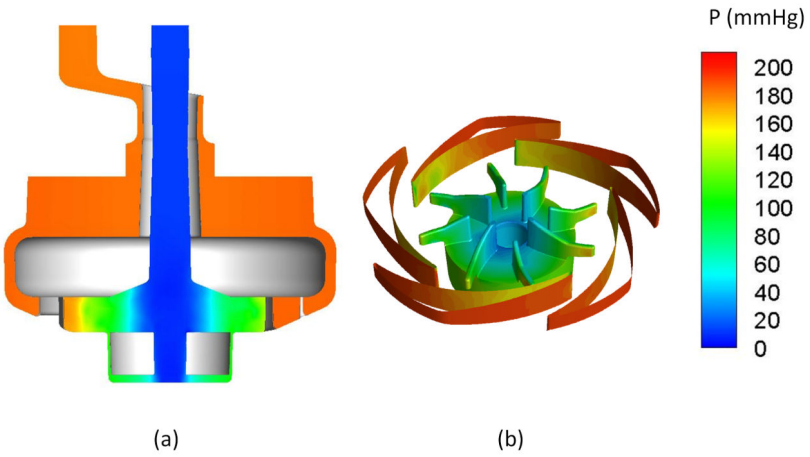

Figure 4.

Computationally predicted pressure distributions within the PediPL device. (a) CFD simulated pressure (on a scale of 0-200 mmHg) through a central planar cut through the device at a flow rate of 1 LPM and an impeller rotation speed of 3000 rpm. (b) Pressure distribution through the impeller and diffuser fins.

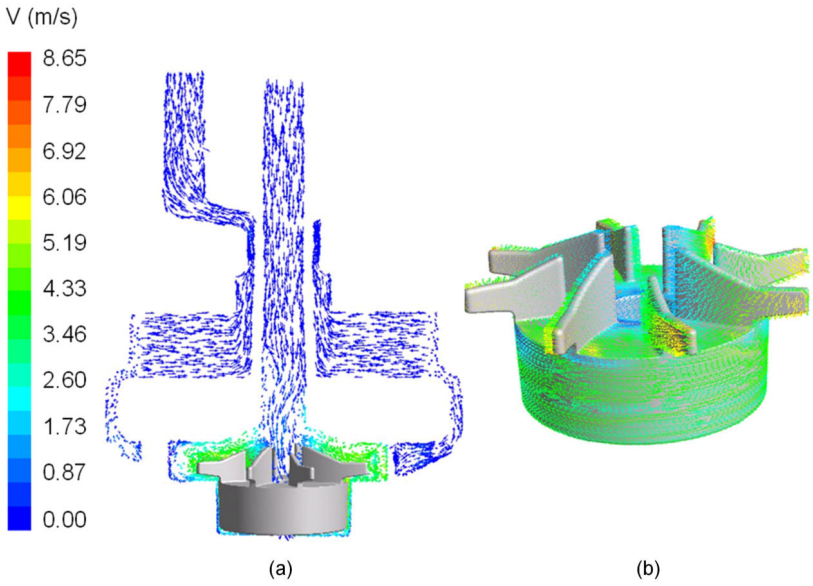

Figure 5.

(a) Flow velocity through the PediPL device at the sectional view; and (b) the near wall velocity vectors on the impeller/rotor.

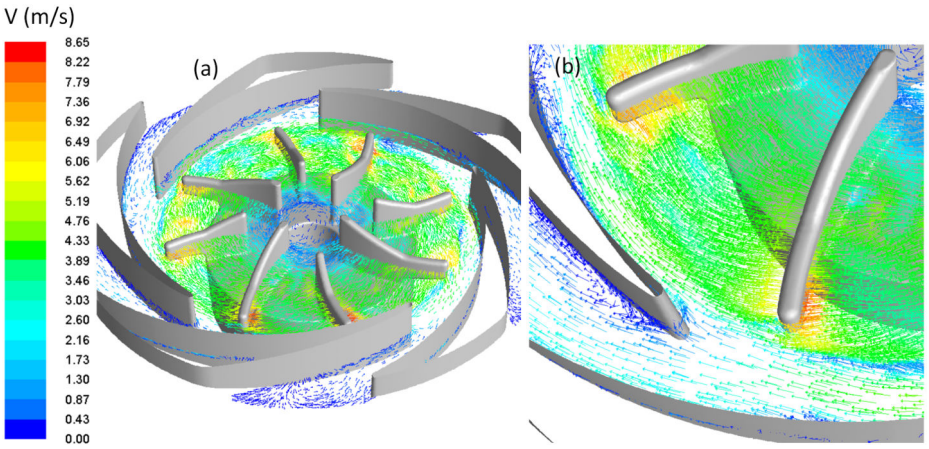

Figure 6.

(a) Flow velocity field on the cut plane through the middle blade cut plane; and (b) enlarged view of the detailed velocity field in the region near the impeller blade tips and diffuser fins.

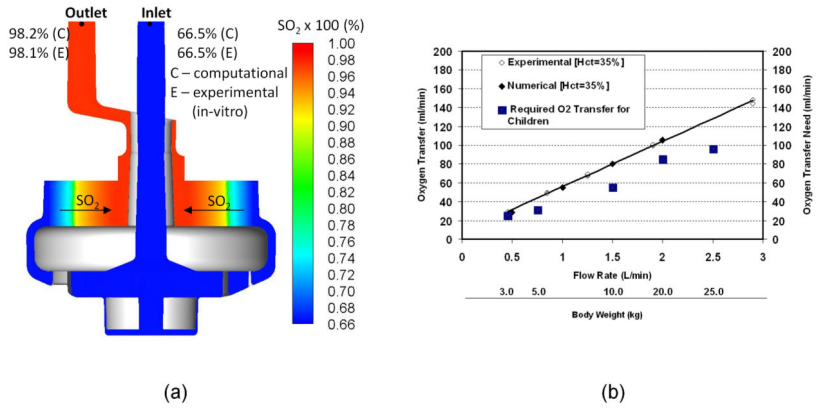

Figure 7.

(a) CFD simulated oxygen saturation distribution compared with in-vitro measured inlet/outlet values at a blood flow of 1 L/min at a rotational speed of 3000 rpm; and (b) the overall oxygen transfer performance of the PediPL device and the required oxygen transfer versus body weight for children.

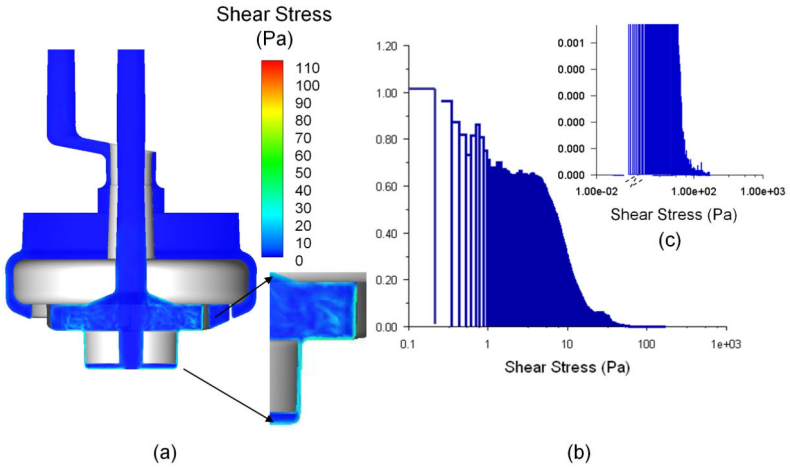

Figure 8.

(a) Shear stress distribution on the central cut plane through middle-plane of the pump-oxygenator (1 LPM, 3000 rpm); and (b) Mass weighted distribution of the shear stresses. (c) Mass weighted distribution of the high shear stresses.

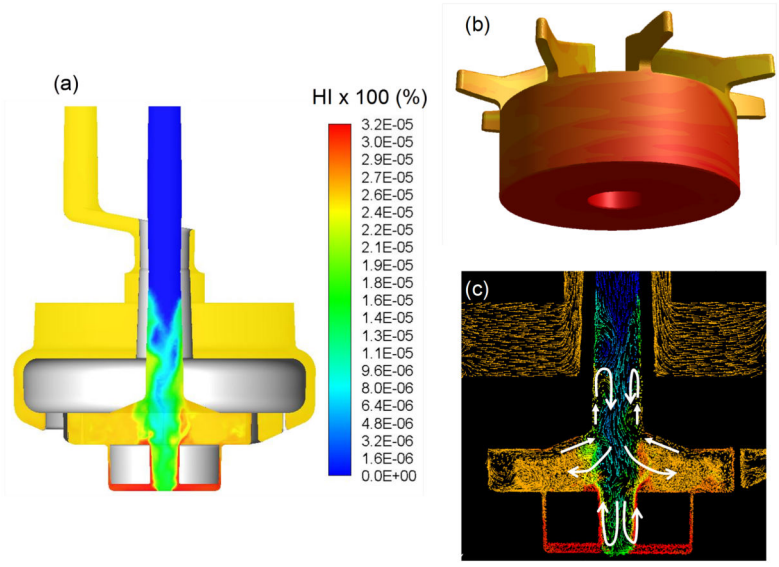

Figure 9.

(a) Hemolysis index (HI) distribution through the central cut plane through the PediPL at a flow rate of 1 L/min at a speed of 3000 rpm; (b) HI distribution on the impeller/rotor component of the device. The highest hemolysis is observed at the bottom of the device around the rotor; (c) The velocity vector fields colored by the HI values presented on the centerline cut plane (white guidance arrows are drawn to emphasize the significant flow features).

Table 1

Comparison of Oxygen Transfer Performance of the PediPL with Commercial Pediatric Oxygenators

Device	Membrane Surface Area (m^2)	Rated Flow (L/min)	Intended Use
PediPL	0.30	2.5	Pediatric Patients
Medtronic Minimax	0.80	2.3	Pediatric Patients
Sorin Dideco KIDS D100	0.22	0.7	Infant
Sorin Dideco KIDS D101	0.61	2.5	Child
Medos Hilite 800 LT	0.32	0.8	Infant
Medos Hilite 2400 LT	0.65	2.4	Child
Terumo CAPIOX® RX05	0.50	1.5	Pediatric

The rated flow is defined as the maximum blood flow rate at which an oxygenator is able to fully saturate the normal venous blood , i.e., 65% to >95%.

Table 2

Comparison of Hemolytic Performance of the PediPL with Other Circulatory Assist Devices and Oxygenators

Device	Hemolysis NIH (g/100L)	Operating Condition	Blood	Source
PediPL	0.040 0.065	2.5 L/min, 3200 rpm, 100 mmHg 1.0 L/min, 3000 rpm, 100 mmHg	Bovine	Measured
Levitronix CentriMag (R) Blood Pump	0.0029	5.0 L/min, 4000 rpm, 350 mmHg	Bovine	Ref. [17]
Levitronix CentriMag (R) Blood Pump	0.036	5.0 L/min, 4000 rpm, 340 mmHg	Bovine	Measured
Integrated Maglev Pump Oxygenator	0.04	5.0 L/min, 3000 rpm, 125 mmHg	Bovine	Ref. [6]
Medtronic BP 80 Pump	0.004	5.0 L/min against 100 mmHg, Rotational Speed (unspecified)	Human	Ref. [18]
Medtronic BP 50 Pump	0.058	0.4 L/min, 2750 rpm, 250 mmHg	Bovine	Ref. [19]
TandemHeart Pump	0.046	0.4 L/min, 5500 rpm, 250 mmHg	Bovine	Ref. [19]
Sorin Dideco Pediatric Oxygenator + Gyro centrifugal pump	0.0253	1.0 L/min, 100 mmHg, Rotational Speed (unspecified)	Bovine	Ref. [20]
Pumping Assist Lung	0.389	500 ml/min, 22 mmHg, 1000 rpm	Bovine	Ref. [21]